AIAA JOURNAL
Vol. 39, No. 3, March 2001

Directional Suppression of Noise from a High-Speed Jet

Dimitri Papamoschou* and Marco Debiasi†
University of California, Irvine, Irvine, California 92697-3975

Experiments demonstrate directional suppression of noise from a high-speed jet using an asymmetric parallel secondary stream. The secondary stream attenuates Mach wave radiation in the lower hemisphere of the acoustic far field, leaving unaltered the upward-propagated Mach waves. An eccentric nozzle arrangement with a Mach 1.5, 700-m/s inner stream and a Mach 1.0, 360-m/s outer stream produces noise reduction superior to that from concentric arrangements or from the fully mixed equivalent jet. The angle of peak perceived noise shifts from the aft quadrant to the lateral direction. The benefit of the eccentric arrangement is attributed to its shorter potential core relative to a concentric jet. The experiments also reveal emission of strong crackle from the untreated jet, a noise component arising from the nonlinearity of Mach waves. The secondary flow suppresses crackle.

I. Introduction

EFFICIENT suppression of noise from high-speed jets is a prerequisite for development of next-generation supersonic transports, which will need to conform to the same takeoff and landing noise regulations that apply to subsonic aircraft.[1] Supersonic jet noise consists of three main components: turbulent mixing noise, comprising the contribution of large-scale and fine-scale structures; broadband shock noise; and screech tones.[2] The latter two are present in imperfectly expanded jets and can be theoretically eliminated by pressure matching the jet. Mixing noise is by far the most difficult to control. For exhaust speeds greater than about 450 m/s, large-scale mixing noise manifests itself primarily as Mach wave radiation, caused by the supersonic convection of turbulent eddies with respect to the ambient. In the vicinity of the potential core, Mach waves are strong, nonlinear pressure waves that decay into weak acoustic waves far from the jet. In high-speed hot jets, Mach wave emission is the dominant source of sound and radiates in the aft quadrant.

The simplest way to explain Mach wave radiation is to consider the turbulent interface between the jet and the ambient as a wavy wall propagating at a convective speed U_c. When U_c is supersonic, Mach waves are radiated from the wall. The notion of sound radiation from large-scale flow instabilities was first confirmed in the supersonic jet experiments of McLaughlin et al.[3] and the subsequent experiments of Troutt and McLaughlin.[4] In those experiments, the orientation, wavelength, and frequency of the measured acoustic radiation were found to be consistent with the Mach wave concept just outlined. The linear stability analysis of Tam and Burton[5] further solidified this idea by showing that the sound emitted by a supersonic instability wave matched very well the aforementioned experimental data. Since then, a large volume of experimental and theoretical works have addressed multiple aspects of this problem (see, for example, Refs. 6–9).

Most silencing efforts for supersonic jets have focused on mixing enhancement, occasionally combined with ejectors. Examples are the works by Westley and Lilley[10] and Seiner and Gilinski[11] on lobed nozzles; Ahuja and Brown,[12] Samimy et al.,[13] and Seiner and Grosh[14] on tabs; Samimy et al.[15] on nozzle cutouts; and Strykowski et al.[16] on a counterflow method. The underlying principle is to enhance the axial decay of the velocity in the jet plume, hence reducing the length of the Mach wave emitting region; at the same time, all of the other sources of noise that depend on jet velocity (fine scale, quadrupole) would also be reduced. Although such methods can produce a significant increase in the jet spreading rate, reduction of mixing noise has been modest at best, and occasionally the jet becomes louder. Moreover, the thrust loss induced by mechanical mixers in supersonic jets can easily reach the order of 10% (Refs. 14 and 17), which is unacceptable for the economic operation of an aircraft. Currently, the leading suppressor is the mixer ejector,[18] which decelerates the jet exhaust by mixing it with entrained air inside a shroud. It provides very good noise reduction, but the required shroud is very large, which adds significant drag and weight penalties on top of the mixer losses.

Recently, it was shown that the addition of a secondary flow (coflow) around a supersonic jet can significantly reduce Mach wave emission.[19,20] The conditions (speed and temperature) of the secondary flow are such as to render the motion of the jet eddies subsonic relative to the secondary flow, while maintaining the secondary-flow eddies subsonic relative to the ambient flow. The jet instability wave becomes intrinsically subsonic, even though the absolute speed of the instability, as seen by a fixed observer, remains supersonic. The method is called Mach wave elimination (MWE) because it prevents formation of strong shock/expansion waves around the jet eddies, which farther out become Mach waves. The conditions of the secondary flow for MWE are based on empirical models for the convective velocity U_c, derived from direct measurements of U_c in jets and shear layers.[21,22]

The effectiveness of the coflow in reducing Mach waves depends primarily on the following factors:

1) The convective Mach number of the jet eddies relative to the coflow, which should be subsonic; the lower its value, the faster the attenuation of the pressure fluctuation within the coflow layer.

2) The coflow thickness; the larger it is, the more room a disturbance has to decay subsonically before it is transmitted to the ambient fluid.

3) The coverage of the Mach wave emitting region of the jet by the coflow; if the coflow mixes fully with the jet before the end of this region, Mach waves will still be generated.

There is a natural conflict between the first two factors and the third one. Application of a coflow around a jet reduces the jet growth rate, thus, it prolongs the Mach wave emitting region of the jet. Early tests of MWE with thin coflows showed little or no far-field noise reduction, even though the near-field noise was suppressed considerably. This is because the coflow stretched the Mach wave emitting region past the point where the coflow was fully mixed with the jet. As a result, Mach waves far from the jet exit escaped treatment. With thicker coflows, an appreciable far-field reduction was obtained,[20] but the diameter and mass flow rate of the coflow became seemingly large for supersonic engine operation.

The special nature of supersonic jet noise offers a possible solution to this dilemma. Mach wave radiation is directional. As far as aircraft noise is concerned, only radiation toward the ground matters. It is, thus, compelling to examine what happens if only the lower part of the jet is treated with a coflow and the upper part is allowed to grow naturally and emit Mach waves toward the heavens.

Received 24 January 2000; revision received 7 August 2000; accepted for publication 7 August 2000.

*Professor, Department of Mechanical and Aerospace Engineering. Senior Member AIAA.

†Postgraduate Researcher, Department of Mechanical and Aerospace Engineering. Member AIAA.

With our present hardware, we were able to set up easily an eccentric dual-stream jet that produced unique and promising results that will help refine this approach in the future. We know of only one previous silencing method that was directional, the thermal acoustic shield (TAS), reviewed by Seiner and Krejsa.[1] The TAS relied on a layer of hot and slow air to reflect/refract acoustic radiation emitted by the jet. At static conditions, it produced a 5-dB drop in perceived noise level in the direction of peak emission. At forward flight, however, the layer dissipated quickly and the acoustic benefit was completely lost. The TAS configuration bears an external, superficial resemblance to the configuration of MWE discussed in this paper. However, the principles of operation and resulting noise attenuation are very different.

The framework of our research is reduction in perceived noise, which is different from absolute noise, using flow configurations that are efficient and realistic from a propulsion standpoint. Included in this effort is suppression of an annoying component of noise, crackle, which is not captured by conventional noise metrics and has been overlooked by recent studies in this field. Within the limitations of our facility, we tried to achieve configurations that approach the exhaust conditions of a realistic turbofan engine appropriate for a Mach 1.8–2.0 transport. This means a jet exhaust velocity around 700 m/s, a jet nozzle pressure ratio around 4, and a fan bypass ratio less than 1.0. In contrast with previous works on Mach wave elimination, the secondary flow was exhausted at conditions that simulate an unheated fan stream.

II. Experimental Setup

A. Apparatus

Experiments were conducted using a dual-stream round jet apparatus depicted in Fig. 1. The primary stream was expanded through an inner supersonic nozzle designed by the method of characteristics for Mach number 1.5. The exit diameter of the inner nozzle was 12.7 mm and its lip thickness was 0.4 mm. Two conical outer nozzles with exit diameters of 17.8 and 21.6 mm were used for the coflow stream. Mixtures of helium and air were supplied to both the primary and secondary streams, which exhausted into ambient still air. By regulating the mass fractions of helium and air, thereby regulating the gas constant of the mixture, we controlled the jet velocity at fixed Mach number. Helium–air mixtures simulate adequately the density, velocity, and speed of sound of a heated jet.[23] One can easily match exactly the velocity and Mach number of a heated jet, in which case there will be a small mismatch in density due to the difference in specific heat ratio between air and the helium–air mixture. For our baseline jet, described hereafter the density mismatch was 9%. Given the weak dependence of shear layer spreading rate on density ratio,[24] we expect this mismatch to have little or no impact on the fluid mechanics of the jet. The facility was instrumented with pressure transducers (Setra Model 280) recording the total pressures in the primary and coflow streams as well as the centerline pitot pressure. A 150-mm-diam schlieren system, illuminated by a 20-ns spark gap (Xenon Model N787B), provided flow visualization.

B. Flow Conditions

The geometry of the jets is summarized in Fig. 1. The baseline jet was pressure matched and had exit velocity $U_1 = 700$ m/s and Mach number $M_1 = 1.5$. The gas constant of the helium–air mixture supplied to the jet was $R = 760$ J/kg · K, and its specific heat ratio was $\gamma = 1.56$. Without coflow, this jet is denoted single. For all cases with coflow, the coflow had exit Mach number $M_2 = 1.00$ and velocity $U_2 = 360$ m/s. The exit density of the coflow was 10% below that of the ambient air, simulating the exhaust of an unheated fan airstream supplied by a compressor with efficiency of 85%, that is, the exhaust temperature of the simulated air stream is 10% above ambient. The eccentric case (ECC) resulted from the misalignment of the 12.7-mm-diam jet nozzle with the 17.8-mm-diam coflow nozzle. For this configuration, the maximum coflow thickness was 4.3 mm, and sound measurements were performed for different values of the azimuthal angle ϕ. Coax1 is a coaxial arrangement having the same coflow area as ECC; it used the same nozzles and had identical thrust and mass flow rates as ECC. Coax2 is a coaxial jet with approximately the same coflow thickness as the maximum coflow thickness in ECC. It used the larger coflow nozzle of 21.6 mm. Finally, there is the fully mixed equivalent (FMEQ) jet of ECC/coax1. Scaled to the same thrust as ECC/coax1, FMEQ has the same mass flow rate and same total enthalpy as ECC/coax1. Tanna[25] has argued that the FMEQ jet is the standard against which dual-stream jets should be judged in the context of noise. A balance of mass, momentum, and total enthalpy shows that the FMEQ has Mach number 1.29 and velocity 550 m/s. Because a Mach 1.29 nozzle was unavailable, this jet was created by operating the Mach

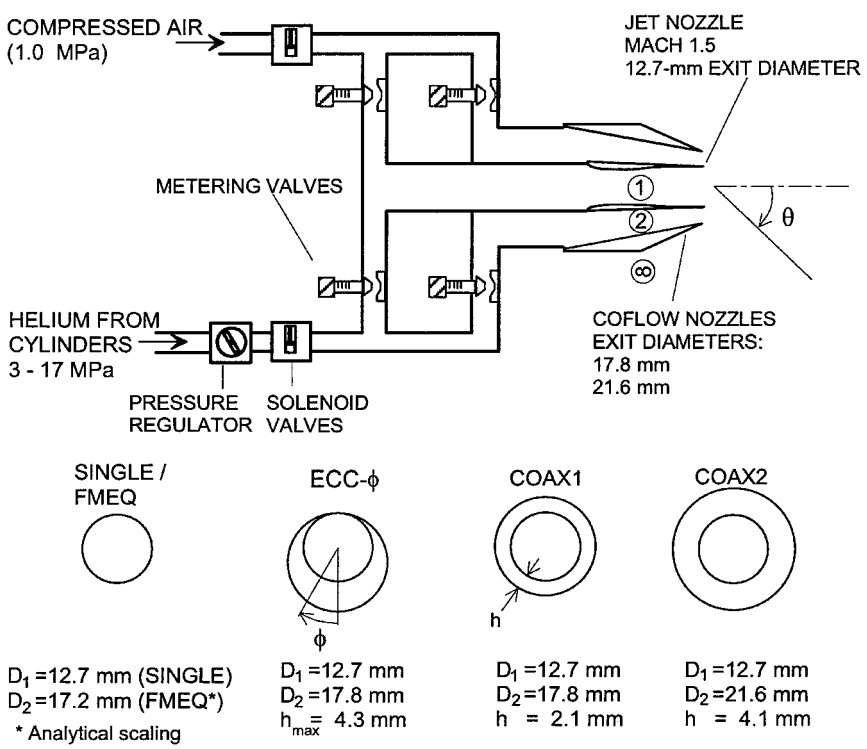

Fig. 1 Experimental facility and geometry of cases studied.

Table 1 Flow conditions[a]

Case	M_1	U_1	ρ_1/ρ_∞	M_2	U_2	$\dot{m}_2/\dot{m}_1$	M_c	F/F_{single}
Single	1.50	700	0.59	——	——	——	1.60	1.00
ECC-ϕ	1.50	700	0.59	1.00	360	0.67	0.41	1.35
Coax1	1.50	700	0.59	1.00	360	0.67	0.41	1.35
Coax2	1.50	700	0.59	1.00	360	1.45	0.41	1.73
FMEQ	1.29	550	0.91	——	——	——	1.25	0.70

[a] U in m/s, F denotes thrust, and ϕ is azimuthal angle of microphone.

1.5 nozzle in overexpanded mode, resulting in an isentropically expanded Mach number of 1.29. The overexpansion created screech tones that would not have occurred if the jet were pressure matched. This entailed special handling of the noise spectra, described later, for meaningful comparisons with the other cases.

Table 1 summarizes the flow conditions. The next-to-last column lists the convective Mach number of the jet eddies M_c relative to their surrounding fluid (ambient in single and FMEQ, coflow in all others). M_c was predicted using the empirical model of Murakami and Papamoschou,[22] which is based on experimental measurements of the eddy convective velocity. The last column lists the calculated thrust of each case normalized by the thrust of case single; this ratio is used for equal-thrust scaling of the noise data. The Reynolds number of the primary jet, based in D_1, was 3.5×10^5 for the first four cases and 3.3×10^5 for FMEQ.

C. Noise Measurement

The jet noise was recorded by a 1/8-in. condenser microphone connected to a preamplifier and power supply (Bruel and Kjaer Models 4138, 2670, and 5935L, respectively). It was calibrated daily before each series of recordings (Bruel and Kjaer Model 4231 calibrator). Sound measurements were conducted inside an anechoic chamber, approximately 8 m^3 in volume, lined with acoustic wedges (Sonex). The microphone was mounted on an arm that pivoted around an axis, passing through the center of the jet exit. This study concerns itself only with the far-field sound, for which the microphone was moved on an arc of radial distance $r = 1.02$ m ($r/D_1 = 80$). The polar angle θ (Fig. 1) ranged from 20 to 100 deg, measured clockwise from the jet axis. (Because most measurements were done in the lower hemisphere, this convention obviates the need to use negative values for θ throughout this paper.) A few measurements were performed in the upper hemisphere. The azimuthal angle ϕ took the values of 0, 30, and 45 deg with respect to the vertical; obviously, this pertains only to the ECC. The relative humidity and temperature of the ambient air inside the anechoic chamber were recorded during each experiment.

The microphone, which has a frequency response of 150 kHz, was sampled at 400 kHz by a fast analog-to-digital board (National Instruments AT-MIO-16E1) installed in a Pentium Pro computer. Each recording consisted of 54,280 samples (135 ms), corresponding to the passage of about 10,000 eddies the size of the inner-jet diameter. The signal was high-pass filtered at 500 Hz by a Butterworth filter to remove spurious low-frequency noise. The narrowband power spectrum of the microphone voltage was computed using a 2048-point fast Fourier transform, which provided a spectral resolution of 195 Hz. By the use of the microphone's sensitivity of 1 mV/Pa and accounting for the amplifier gain setting, the voltage power spectrum was converted to the power spectrum of p'/p_{ref}, where p' is the pressure fluctuation and $p_{\text{ref}} = 20$ μPa is the commonly used reference pressure. Converted to decibels, this becomes the spectrum of the sound pressure level (SPL), $\text{SPL}_{\text{raw}}(f)$, where f is the measured frequency. This spectrum must undergo several corrections before accurate data can be extracted. The corrected spectrum is given by

$$\text{SPL}(f) = \text{SPL}_{\text{raw}}(f) - C_{\text{fr}}(f) - C_{\text{ff}}(f) + \alpha(f)r - 10\log_{10}(F/F_{\text{single}}) \tag{1}$$

where C_{fr} and C_{ff} are the corrections for the actuator response and free-field response, respectively; they are based on data provided by the manufacturer of the microphone. The atmospheric absorption coefficient is α (in decibels per meter), computed using the formulas proposed by Bass et al.[26] for the measured values of relative humidity and temperature of the ambient air. At a relative humidity of 30% (typical in our runs), the absorption correction at $f = 100$ kHz and $r = 1$ m is 2.5 dB. The last term scales all of the results to the same thrust level. The overall sound pressure level (OASPL) was obtained by integrating the corrected spectrum:

$$\text{OASPL} = 10\log_{10}\int_0^{f_{\text{upper}}} 10^{0.1\,\text{SPL}(f)}\,\mathrm{d}f \tag{2}$$

where the upper limit is the highest frequency that can be resolved, in this case, 150 kHz.

Assessment of noise reduction schemes is inextricably connected with the human perception of sound, which is very sensitive to the frequency content of the acoustic signal. OASPL is an inadequate and potentially misleading metric in this respect because, as its name implies, it describes only the overall sound, not its distribution vs frequency. Noise sources with the same OASPL can be as much as 17 dB apart in perceived noise, depending on their spectral content.[27] Noise from subscale experiments must be scaled up to full size for meaningful assessment of perceived noise. The corresponding full-size frequencies f^* are obtained by dividing the frequencies measured in the experiment by the scale factor, $f^* = f/\text{scale}$. To scale up the results of our experiment to an engine exhaust diameter of 1 m, a scaling factor of 80 was used. To proceed further, the scaled-up narrowband spectrum must be converted to a discrete third-octave spectrum because all aircraft noise metrics are based on third-octave analysis. The center frequency of the kth octave (OCT_k) band is determined by $f^*_{\text{oct},k} = 2^{1/3} f^*_{\text{oct},k-1}$, with $f^*_{\text{oct},1} = 10$ Hz. The lower and upper limits of band k are $2^{-1/6} f^*_{\text{oct},k}$ and $2^{1/6} f^*_{\text{oct},k}$, respectively. The SPL in band k is obtained by integrating the narrowband SPL spectrum as follows:

$$\text{OCT}_k = 10\log_{10}\int_{2^{-\frac{1}{6}} f^*_{\text{oct},k}}^{2^{\frac{1}{6}} f^*_{\text{oct},k}} 10^{0.1\,\text{SPL}(f^*)}\,\mathrm{d}f^* \tag{3}$$

A simple metric for the human reaction to noise is the A-weighting, which adds a standard correction curve to the third-octave spectrum:

$$\text{dBA}_k = \text{OCT}_k + A\text{-weight}_k \tag{4}$$

The correction is, for example, -70.4 dB for 10 Hz, -19.1 dB for 100 Hz, -3.2 dB for 500 Hz, 0 dB for 1000 Hz, and $+1.2$ dB for 2000 Hz. The frequencies above 1000 Hz weigh heavily in this metric. The same is true for all other forms of perceived noise metrics, such as perceived noise level (PNL), effective PNL (EPNL), etc.[27] In subscale jets two orders of magnitude smaller than the engine exhaust, such as ours, noise at frequencies below 10,000 Hz is of little significance to aircraft noise.

III. Results

A. Flow Visualization

Figure 2 presents spark schlieren photographs of cases single, ECC-0, coax1, and FMEQ. The Mach waves of single are evident; their Mach angle is $\mu \approx 40$ deg, indicating a convective Mach number $M_c = 1/\sin\mu \approx 1.56$, which is consistent with the prediction of 1.60 in Table 1. Application of the coflow in case coax1 eliminates most Mach waves near the nozzle, but some Mach waves far from the nozzle are still apparent. Recall the argument in the Introduction about the lengthening of the potential core with application of the coflow. In case ECC-0, the lower hemisphere appears very clean and devoid of Mach waves, whereas radiation is unaltered in the upper hemisphere. The FMEQ jet emits Mach wave radiation, although it is weaker in the case single.

B. Centerline Mach Number

Figure 3 shows the centerline Mach number distributions for cases single, coax1, coax2, and ECC. The lengthening of the jet with application of the concentric coflows is evident. Although it is not easy to infer potential core lengths from Fig. 3, we can concentrate on, for example, the length to $M = 1$, which is probably more relevant to Mach wave emission. With reference to single, this length is

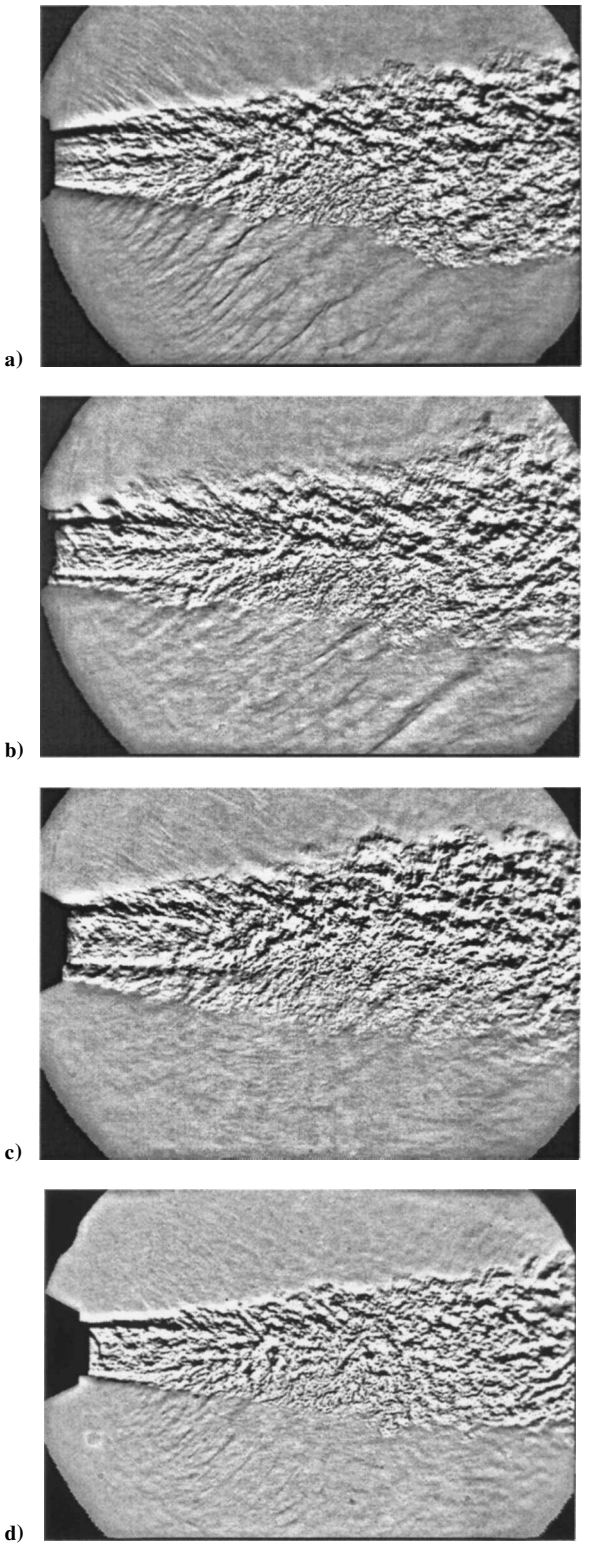

Fig. 2 Spark schlieren images of a) single, b) coax1, c) ECC-0, and d) FMEQ.

stretched 24% in coax1 and 45% in coax2. In contrast, the eccentric arrangement ECC stretches the $M = 1$ length by only 6%. It is evident that the eccentric flow mixes faster than the concentric flows and approaches the mixing rate of the single jet.

C. Actual Noise

The directional treatment of case ECC created very different upper and lower acoustic fields. Shown in Fig. 4 are the far-field spectra of ECC-0 at the angles of $\theta = -40$ deg (upward) and $\theta = +40$ deg (downward). They are compared with the spectra of case single. In

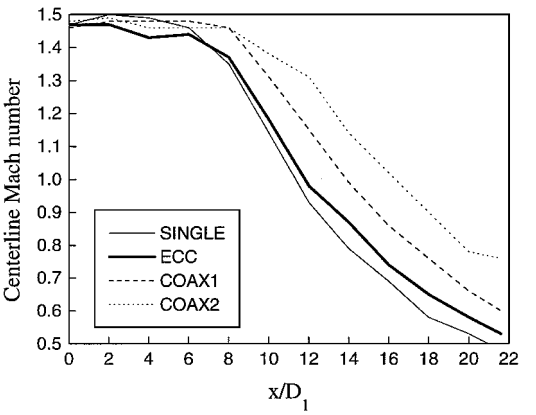

Fig. 3 Centerline Mach number distributions vs normalized axial distance.

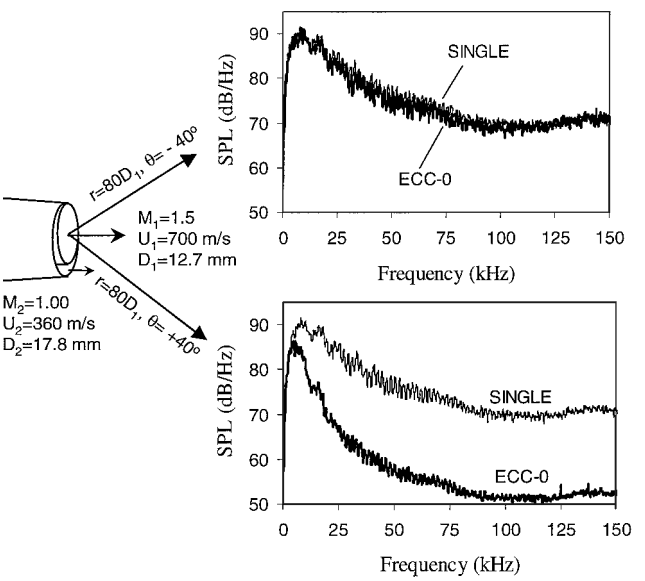

Fig. 4 Narrowband spectra of ECC-0 at the angles $\theta = \pm 40$ deg with comparison to the spectra of single.

the lower hemisphere there is a moderate reduction, around 5 dB, of the low-frequency components and a substantial reduction, around 18–20 dB, of the frequencies above 50 kHz. The broadband nature of the sound reduction reflects that Mach waves are generated from a large variety of turbulent scales, from very small eddies near the jet exit to very large eddies near the end of the potential core. In the upper hemisphere, the spectra of single and ECC practically overlap. The OASPL was reduced by 7 dB in the downward direction, with no reduction in the upward direction. From this point on the discussion of ECC spectra will relate to the lower hemisphere.

Figure 5 compares the far-field spectra of single, ECC-0, coax1, coax2, in the direction of peak emission, $\theta = 45$ deg. The superiority of the eccentric case is evident, which for $f = 100$ kHz gives a reduction of 18 dB. At the same frequency, coax1, the coaxial jet with same coflow conditions as ECC, gives only a 4-dB reduction. In terms of acoustics, comparison of ECC to coax1 is not fair because coax1 has half the coflow thickness of ECC-0. However, it is a valid comparison in terms of optimizing the exhaust configuration of a turbofan engine with fixed bypass ratio. Acoustically, the fairest comparison is with coax2, which has approximately the same coflow thickness as the maximum thickness of ECC. If ECC and coax2 had the same jet growth rate, they should have produced the same noise benefit. Clearly they do not; ECC has a 10-dB advantage over coax2, even though the coflow mass flow rate in coax2 is 2.2 times that of ECC. This underscores the profound effect of growth rate suppression on Mach wave emission. The shortening of the potential core by 39% (Fig. 3) caused a 10-dB noise benefit.

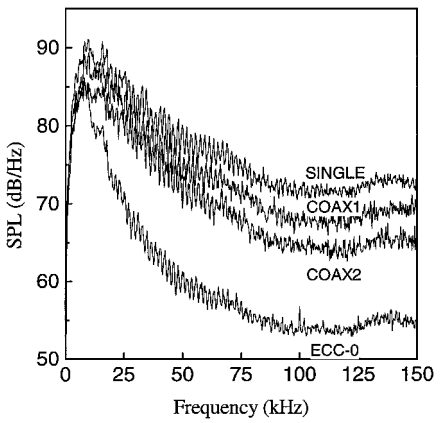

Fig. 5 Narrowband spectra in the direction of peak OASPL ($\theta = 45$ deg) for single, coax1, coax2, and ECC-0.

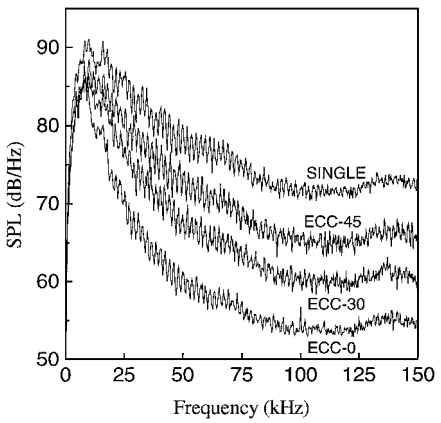

Fig. 6 Narrowband spectra in the direction of peak OASPL ($\theta = 45$ deg) for single, ECC-0, ECC-30, and ECC-45.

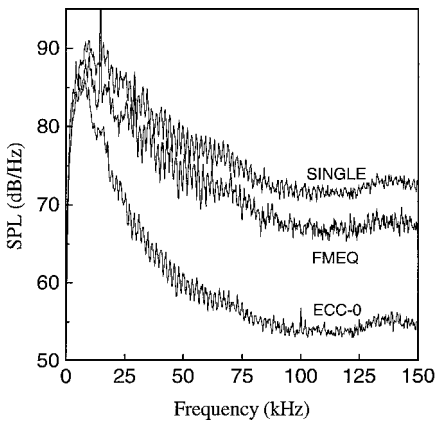

Fig. 7 Narrowband spectra in the direction of peak OASPL for single ($\theta = 45$ deg), ECC-0 ($\theta = 45$ deg), and FMEQ ($\theta = 30$ deg).

Remaining at the same polar angle, Fig. 6 shows the spectra of ECC at the azimuthal angles $\phi = 0$, 30, and 45 deg, and compares them to the spectrum of single. As can be expected from the geometry of the ECC nozzle, the noise benefit declines with increasing ϕ. Even though the benefit at $\phi = 30$ deg is still substantial (13 dB at 100 kHz), the benefit at $\phi = 45$ deg approaches that of coax2 (8 dB at 100 kHz). Relative to the maximum coflow thickness at $\phi = 0$ deg, the coflow thickness at $\phi = 30$ deg is 91% and at $\phi = 45$ deg is 81%. The eccentric arrangement is just the first step in our study of asymmetric coflows and more effective nozzle designs will be explored in the future. Finally, Fig. 7 compares the spectra of single, ECC-0, and FMEQ in the direction of peak noise, which for FMEQ was $\theta = 30$ deg. FMEQ gives a modest noise reduction of about 5 dB at 100 kHz, and its spectrum is very similar to that of coax1 in Fig. 5.

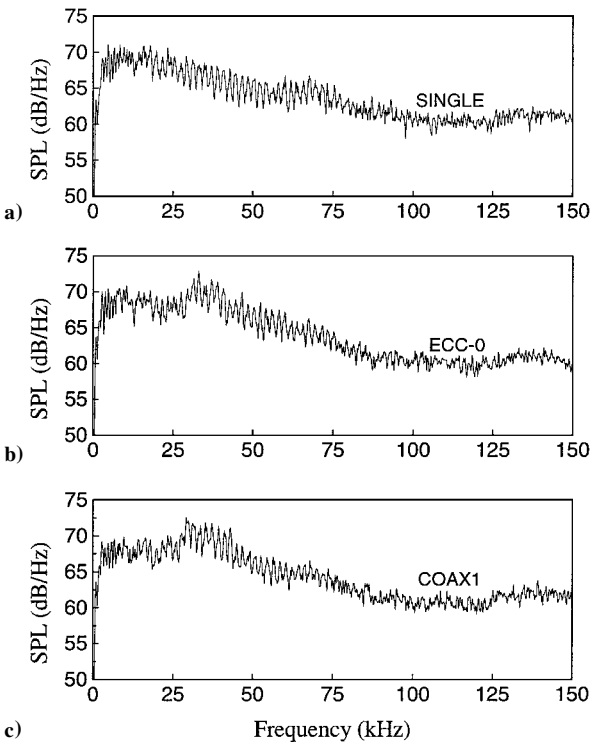

Fig. 8 Narrowband spectra in the lateral direction $\theta = 90$ deg for a) single, b) ECC-0, and c) coax1.

The ECC is superior to FMEQ, even at $\phi = 45$ deg. The reason for the ineffectiveness of FMEQ in reducing noise is that, despite its lower velocity relative to single, it still radiates Mach waves as evidenced in Fig. 2d. The spectrum of FMEQ has sharp peaks at 15 and 30 kHz, which are the screech tones due to overexpansion of this jet. Earlier research has shown that, except for these tones, the aft-quadrant spectra of imperfectly matched jets are identical to those of perfectly expanded jets with the same fully expanded velocity and Mach number.[28] To obtain fair representations of the third-octave and dBA spectra of FMEQ, the screech tones were removed manually from all of the FMEQ narrowband spectra. This was a straightforward procedure because the tones were very localized. In addition to screech tones, there is also the issue of broadband shock noise, which cannot be removed as conveniently. However, it affects only the lateral and forward directions, in which the jet is much quieter than it is in the aft quadrant; it will have no effect on our evaluations of perceived noise.

Turning now our attention to the noise emission in the lateral direction, Fig. 8 plots the spectra of single, ECC-0, and coax1 at $\theta = 90$ deg. There are no remarkable differences between them; the coflow has no appreciable impact on this noise, which is caused by fine-scale turbulence in the jet. The directivity of OASPL for single, ECC-0, and FMEQ is plotted in Fig. 9. The OASPL peaks at $\theta = 45$ deg for single and ECC-0, and at 30 deg for FMEQ. In terms of net OASPL reduction over the entire arc, ECC-0 gives a 8.5-dB reduction and FMEQ a 3.3-dB reduction.

D. Perceived Noise

Figure 10 plots the dBA spectra of single, ECC-0, and FMEQ in their respective directions of peak emission. At 1000 Hz, ECC-0 provides a reduction of 18 dB, while FMEQ provides a reduction of only 5 dB. The spectral peak, $\mathrm{dBA_{peak}}$, used here as a measure of perceived noise, is reduced by 15 dB in ECC-0 and by 5 dB in FMEQ. The performance of ECC-0 is slightly hurt, in this respect, by a small peak at 200 Hz; better shaping of the coflow nozzle may help in eliminating it. Figure 11 shows the dBA spectra of single and ECC in the azimuthal directions $\phi = 0$, 30, and 45 deg. As noted in the discussion of the narrowband spectra, the geometry of the eccentric nozzle makes noise reduction less effective in the sideline direction. Figure 12 presents the directivity of $\mathrm{dBA_{peak}}$ for single, ECC-0, and FMEQ. Perceived noise peaks at $\theta = 45$ deg for single,

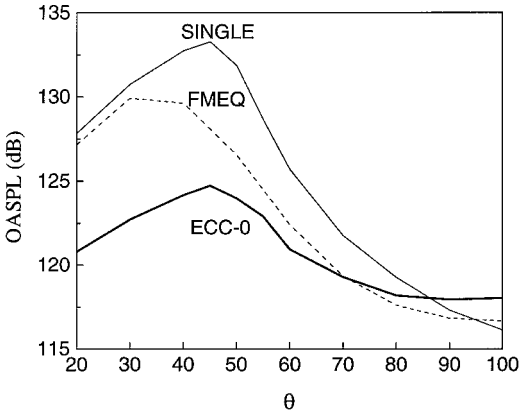

Fig. 9 OASPL vs θ for single, ECC-0, and FMEQ.

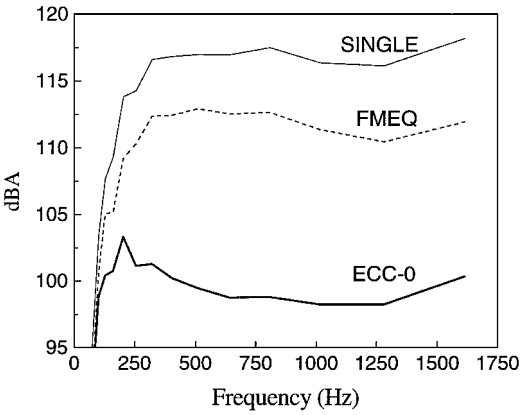

Fig. 10 A-weighted spectra at $\theta = 45$ deg for single and ECC-0, and $\theta = 30$ deg for FMEQ.

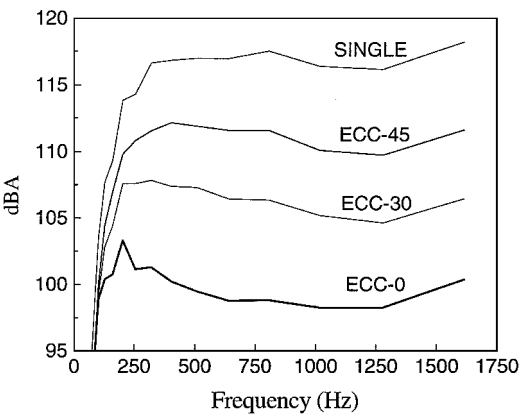

Fig. 11 A-weighted spectra at $\theta = 45$ deg for single, ECC-0, ECC-30, and ECC-45.

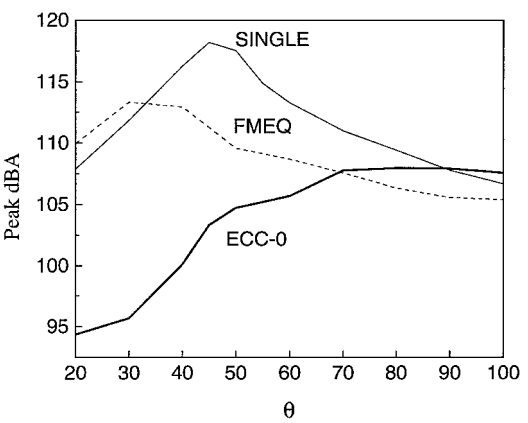

Fig. 12 A-weighted spectral peak vs θ for single, ECC-0, and FMEQ.

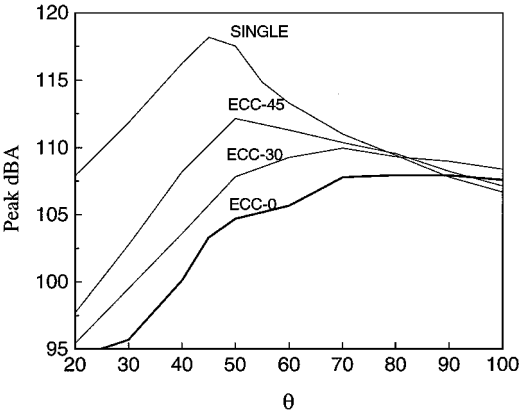

Fig. 13 A-weighted spectral peak vs θ for single, ECC-0, ECC-30, and ECC-45.

$\theta = 30$ deg for FMEQ, and $\theta \approx 80$ deg for ECC-0. Application of the coflow has reduced Mach wave emission so dramatically that the angle of peak perceived noise shifts from the aft quadrant to the lateral direction, which is dominated by mixing noise from fine-scale turbulence. In terms of net perceived noise reduction over the entire arc, FMEQ offers a 5-dB benefit, whereas the benefit of ECC-0 is 11 dB. The $\mathrm{dBA_{peak}}$ directivity of ECC measured at various azimuthal angles is shown in Fig. 13. Compared to single, the net benefit of ECC is 8 dB at $\phi = 30$ deg and 6 dB at $\phi = 45$ deg.

The dBA spectra underscore the limitation of our subscale experiments: the inability to resolve the entire audible spectrum, up to 20 kHz, when we scale up the data. This prevents the calculation of common aircraft noise metrics such as PNL, EPNL, etc. The solution would be to use a microphone with response up to 1 MHz, which does not exist, or scale up the facility by a factor of at least five, a very expensive proposition. Tests in existing, large-scale facilities are, therefore, desirable once an optimum nozzle configuration has been determined in small-scale tests.

E. Nonlinear Effects

This part of the investigation was spurred by a rather unorthodox way of studying noise. The microphone time trace was converted to a digital audio file and played back at 1/80th the recording speed to simulate noise from a 1-m-diam exhaust (the conversion program was instructed that the sampling rate was 5000 $\mathrm{s^{-1}}$ instead of the actual 400,000 $\mathrm{s^{-1}}$). The playback of the untreated jet revealed a sound remarkably similar to the sound of military jet engines. In the direction of peak emission, a striking and very annoying feature of the playback was the random occurrence of popping sounds, akin to miniature explosions. In acoustic terms, this noise is called crackle; it was first studied for supersonic jets by Ffowcs Williams et al.[29] This substantial work examined crackle from full-scale engines and subscale experiments. The authors demonstrated that crackle coincides with Mach wave radiation and is not caused by shocks in the jet plume due to imperfect expansion of the jet. They attributed crackle to the nonlinear wave steepening near the source and argued that long-term nonlinear propagation effects were insignificant. Because spectral analysis cannot capture this transient, abrupt phenomenon, crackle was quantified in terms of the skewness of the probability density function (PDF) of the acoustic signal. Noises with skewness below 0.3 were crackle free, whereas those with skewness above 0.4 crackled distinctly.

We were, thus, compelled to examine our pressure time traces and compute the PDF and its skewness. Figures 14a and 14b show 2.5-ms samples of the raw microphone signal $p'(t)$ in the direction of peak emission for single and ECC-0, respectively. Even though it has zero mean, the time trace of single is skewed toward the positive side, indicating stronger compressions than expansions. This is a sign of nonlinearity of sound propagation: Strong compression waves tend to steepen and form shocks; the associated positive p' events are sharp. In contrast, the negative p' events, associated with expansions, are smoother. Because the time-averaged p' must be zero, this dictates that the positive p' events have larger amplitude than the

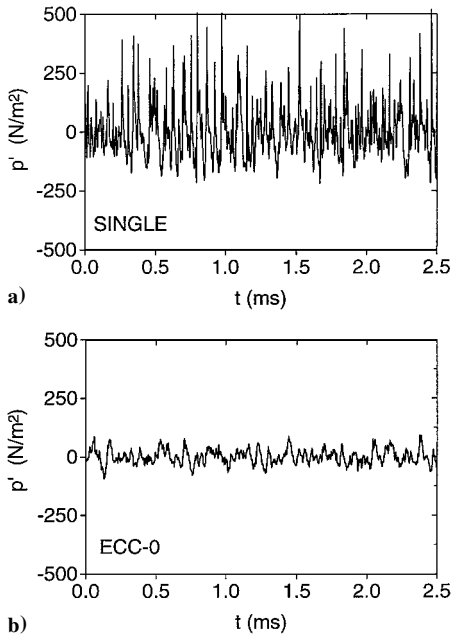

Fig. 14 Samples of microphone time traces measured at $\theta = 45$ deg.

negative ones, which is reflected in the microphone trace. The time trace of ECC-0, on the other hand, is symmetric and with significantly lower amplitude, reflecting the 8-dB drop in OASPL (Fig. 9).

Letting $x = p'/p'_{\text{rms}}$, the distribution function

$$F(\xi) = \mathcal{P}(x \leq \xi) \tag{5}$$

where $\mathcal{P}$ denotes probability, was differentiated to obtain the PDF:

$$\text{PDF}(\xi) = \frac{\mathrm{d}F}{\mathrm{d}\xi} \tag{6}$$

which is plotted in Fig. 15 for single and ECC-0. In the linear plot of Fig. 15a, the PDF of single is skewed toward the positive side, indicating compressions of higher amplitude than expansions. The PDF of single is practically the same as the PDF of noise from the Olympus 593 engine at jet velocity of 622 m/s (Ref. 29). The PDF of ECC-0 is more symmetric and approaches the normal distribution. To see more clearly the probability of high-amplitude events, the PDFs for single and ECC-0 are plotted in logarithmic coordinate in Fig. 15b. For single, positive events (compressions) with amplitude $6p'_{\text{rms}}$ have a probability of 3.2×10^{-4}. Even though this probability looks small, it means that pressure spikes with decibel levels 17 counts above the base signal would be heard every 0.7 s, on the average, from a full-scale engine. Examining the likelihood of $p' = 4p'_{\text{rms}}$, the normal distribution $(2\pi)^{-1/2}\exp(-x^2/2)$ gives a probability 1.3×10^{-4}, the distribution of ECC-0 gives a probability 3.2×10^{-4}, and the distribution of single gives a probability 5.1×10^{-3}, 16 times that of ECC-0.

The skewness Sk (third central moment) of the PDF is

$$\text{Sk} = \int_{-\infty}^{\infty} \text{PDF}(x)(x - \bar{x})^3 \, \mathrm{d}x \tag{7}$$

where the overbar denotes the mean value. The distribution of skewness vs polar angle for cases single, FMEQ, and ECC-0 is shown in Fig. 16. For single and FMEQ, the directivity of skewness coincides with that of dBA_{peak}, indicating once again the strong correlation of sound nonlinearity with Mach wave emission. Single has a peak skewness of 1.2 whereas FMEQ has a peak skewness of 0.8, both well above the crackle criterion of 0.4 proposed by Ffowcs Williams et al.[29] The skewness of ECC-0 is below 0.4 for all angles except $\theta = 55$ deg, where it is barely above 0.4. This indicates that ECC-0 has little or no crackle, consistent with the elimination of Mach waves.

Even though the pressure spikes of crackle occupy a small fraction of the total acoustic energy, they constitute a very annoying component of noise. Despite the good correlation of crackle with skewness,

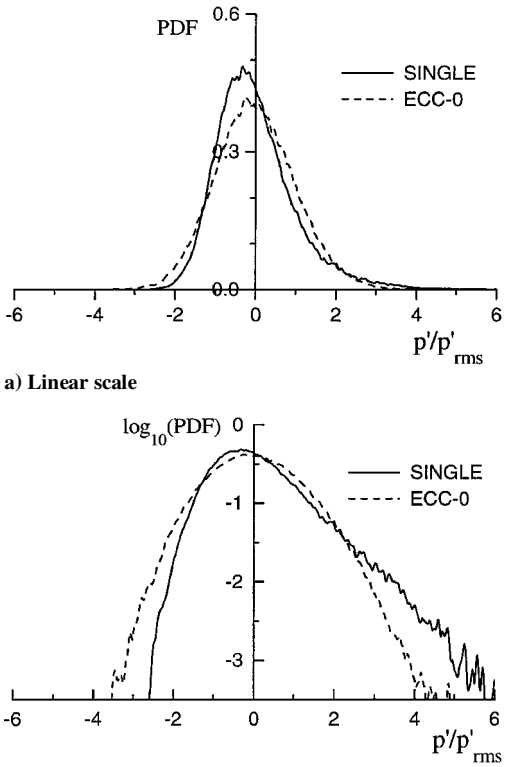

Fig. 15 Probability density function of pressure fluctuation for single and ECC-0.

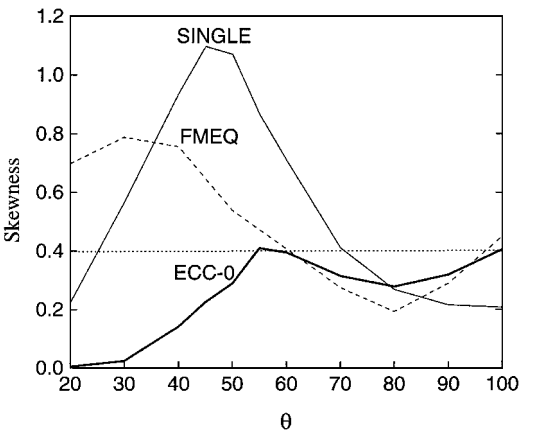

Fig. 16 Directivity of skewness in the noise of single, ECC-0, and FMEQ; dotted line indicates the crackle criterion of Ffowcs Williams et al.[29]

skewness is an incomplete descriptor of this noise because it does not capture the sharpness of the pressure waves, which is the source of the annoyance. Other methods such as wavelet transforms may help quantify better this important aspect of high-speed jet noise.

IV. Conclusions

The far-field, downward-directed sound of a 700-m/s jet was suppressed using an eccentric coflow that eliminated Mach waves from the bottom portion of the jet. The coflow was supplied at a mass flow ratio of 0.67 and at conditions simulating an unheated sonic fan stream. Application of the coflow resulted in a shift of the perceived-noise directivity from the aft quadrant to the lateral direction, with mixing noise from fine-scale turbulence becoming the dominant source of perceived noise. In the aft quadrant, perceived noise was reduced by approximately 16 dBA. Over the measurement arc of 20–100 deg from the jet axis, the net reduction in perceived noise was 11 dBA. Because of its shorter potential core, the eccentric arrangement was superior to coaxial configurations. It also performed

better than the fully mixed equivalent single jet. The experiments also revealed the emission of strong crackle from the untreated jet, a noise component arising from the nonlinearity of Mach waves. Crackle was quantified in terms of the skewness of the probability density function of the recorded noise; it was also evident as sharp positive pressure spikes in the microphone time traces. The coflow suppressed crackle, consistent with elimination of Mach waves.

Acknowledgment

The support by NASA Langley Research Center is gratefully acknowledged (Grant NAG-1-2104, monitored by Thomas D. Norum).

References

[1]Seiner, J. M., and Krejsa, E., "Supersonic Jet Noise and the High-Speed Civil Transport," AIAA Paper 89-2358, 1989.

[2]Tam, C. K. W., and Chen, P., "Turbulent Mixing Noise from Supersonic Jets," *AIAA Journal*, Vol. 32, No. 9, 1994, pp. 1774–1780.

[3]McLaughlin, D. K., Morrison, G. D., and Troutt, T. R., "Experiments on the Instability Waves in a Supersonic Jet and Their Acoustic Radiation," *Journal of Fluid Mechanics*, Vol. 69, Pt. 1, 1975, pp. 73–95.

[4]Troutt, T. R., and McLaughlin, D. K., "Experiments on the Flow and Acoustic Properties of a Moderate Reynolds Number Supersonic Jet," *Journal of Fluid Mechanics*, Vol. 116, March 1982, pp. 123–156.

[5]Tam, C. K. W., and Burton, D. E., "Sound Generated by Instability Waves of Supersonic Flows. Part 2. Axisymmetric Jets," *Journal of Fluid Mechanics*, Vol. 138, Jan. 1984, pp. 249–271.

[6]Seiner, J. M., Bhat, T. R. S., and Ponton, M. K., "Mach Wave Emission from a High-Temperature Supersonic Jet," *AIAA Journal*, Vol. 32, No. 12, 1994, pp. 2345–2350.

[7]Mitchell, B. E., Lele, S. K., and Moin, P., "Direct Computation of Mach Wave Radiation in an Axisymmetric Supersonic Jet," *AIAA Journal*, Vol. 35, No. 10, 1997, pp. 1574–1580.

[8]Fenno, C. C., Bayliss, A., and Maestrello, L., "Interaction of Sound from Supersonic Jets with Nearby Structures," *AIAA Journal*, Vol. 36, No. 12, 1998, pp. 2153–2162.

[9]Mankbadi, R. R., Hixon, R., Shih, S.-H., and Povinelli, L. A., "Use of Linearized Euler Equations for Supersonic Jet Noise Prediction," *AIAA Journal*, Vol. 36, No. 2, 1998, pp. 140–147.

[10]Westley, R., and Lilley, G. M., "An Investigation of the Noise Field from a Small Jet and Methods for Its Reduction," Rept. 53, College of Aeronautics, Cranfield Univ., Cranfield, England, U.K., Jan. 1952.

[11]Seiner, J. M., and Gilinski, M. M., "Nozzle Thrust Optimization While Reducing Jet Noise," *AIAA Journal*, Vol. 35, No. 3, 1997, pp. 420–427.

[12]Ahuja, K. K., and Brown, W. H., "Shear Flow Control by Mechanical Tabs," AIAA Paper 89-0994, 1989.

[13]Samimy, M., Zaman, K. B. M. Q., and Reeder, M. F., "Effect of Tabs on the Flow and Noise Control of an Axisymmetric Jet," *AIAA Journal*, Vol. 31, No. 4, 1993, pp. 609–619.

[14]Seiner, J. M., and Grosch, C. E., "Mixing Enhancement by Tabs in Round Supersonic Jets," AIAA Paper 98-2326, 1998.

[15]Samimy, M., Kim, J.-H., Clancy, P. S., and Martens, S., "Passive Control of Supersonic Rectangular Jets via Nozzle Trailing-Edge Modifications," *AIAA Journal*, Vol. 36, No. 7, 1998, pp. 1230–1239.

[16]Strykowski, P. J., Krothapalli, A., and Jendoubi, S., "The Effect of Counterflow on the Development of Compressible Shear Layers," *Journal of Fluid Mechanics*, Vol. 308, Feb. 1996, pp. 63–96.

[17]Zaman, K. B. M. Q., "Jet Spreading By Passive Control and Associated Performance Penalty," AIAA Paper 99-3505, 1999.

[18]Tillman, T. G., Paterson, R. W., and Presz, W. M., "Supersonic Nozzle Mixer Ejector," *Journal of Propulsion and Power*, Vol. 8, 1992, pp. 513–519.

[19]Papamoschou, D., "Mach Wave Elimination from Supersonic Jets," *AIAA Journal*, Vol. 35, No. 10, 1997, pp. 1604–1611.

[20]Papamoschou, D., and Debiasi, M., "Noise Measurements in Supersonic Jets Treated with the Mach Wave Elimination Method," *AIAA Journal*, Vol. 37, No. 2, 1999, pp. 154–160.

[21]Papamoschou, D., and Bunyajitradulya, A., "Evolution of Large Eddies in Compressible Shear Layers," *Physics of Fluids,* Vol. 4, No. 3, 1997, pp. 756–765.

[22]Murakami, E., and Papamoschou, D., "Eddy Convection in Supersonic Coaxial Jets," *AIAA Journal*, Vol. 38, No. 4, 2000, pp. 628–635.

[23]Kinzie, K. W., and McLaughlin, D. K., "Measurements of Supersonic Helium/Air Mixture Jets," *AIAA Journal,* Vol. 37, No. 11, 1999, pp. 1363–1369.

[24]Brown, G. L., and Roshko, A., "On Density Effects and Large-Scale Structure in Turbulent Mixing Layers," *Journal of Fluid Mechanics,* Vol. 64, No. 4, 1974, pp. 775–781.

[25]Tanna, H. K., "Coannular Jets–Are They Really Quiet and Why?" *Journal of Sound and Vibration*, Vol. 72, No. 1, 1980, pp. 97–118.

[26]Bass, H. E., Sutherland, L. C., Blackstock, D. T., and Hester, D. M., "Atmospheric Absorption of Sound: Further Developments," *Journal of the Acoustical Society of America,* Vol. 97, No. 1, 1995, pp. 680–683.

[27]Smith, M. J. T., *Aircraft Noise*, Cambridge Univ. Press, Cambridge, England, U.K., 1989, pp. 9, 15, 83.

[28]Debiasi, M., and Papamoschou, D., "Noise from Imperfectly Expanded Supersonic Coaxial Jets," *AIAA Journal*, Vol. 39, No. 3, 2001, pp. 388–395.

[29]Ffowcs Williams, J. E., Simson, J., and Virchis, V. J., "Crackle: An Annoying Component of Jet Noise," *Journal of Fluid Mechanics*, Vol. 71, Pt. 2, 1975, pp. 251–271.

M. Samimy
Associate Editor